

Washington University School of Medicine

Digital Commons@Becker

---

2020-Current year OA Pubs

Open Access Publications

---

3-31-2022

## Differential function and maturation of human stem cell-derived islets after transplantation

Kristina G Maxwell

Michelle H Kim

Sarah E Gale

Jeffrey R Millman

Follow this and additional works at: [https://digitalcommons.wustl.edu/oa\\_4](https://digitalcommons.wustl.edu/oa_4)



Part of the [Medicine and Health Sciences Commons](#)

---

# Differential Function and Maturation of Human Stem Cell-Derived Islets After Transplantation

Kristina G Maxwell, Michelle H Kim, Sarah E Gale, Jeffrey R Millman




The advertisement banner features a dark blue background with a green horizontal bar at the bottom. On the left, there is a partial view of a white laboratory instrument. The text is centered and reads: "You Don't Need Reproducible Research UNTIL YOU DO." in white, with "UNTIL YOU DO." in a larger font. Below this, the green bar contains the text "Minimize uncertainty with PHCbi brand products" in white. On the right side of the banner, the PHCbi logo is displayed in blue.

You Don't Need Reproducible Research  
**UNTIL YOU DO.**  
Minimize uncertainty with PHCbi brand products

**PHCbi**

# Differential Function and Maturation of Human Stem Cell-Derived Islets After Transplantation

Kristina G. Maxwell<sup>1,2</sup>, Michelle H. Kim<sup>1</sup>, Sarah E. Gale<sup>1</sup>, Jeffrey R. Millman<sup>1,2,\*</sup> 

<sup>1</sup>Division of Endocrinology, Metabolism and Lipid Research, Washington University School of Medicine, St. Louis, MO, USA

<sup>2</sup>Department of Biomedical Engineering, Washington University in St. Louis, St. Louis, MO, USA

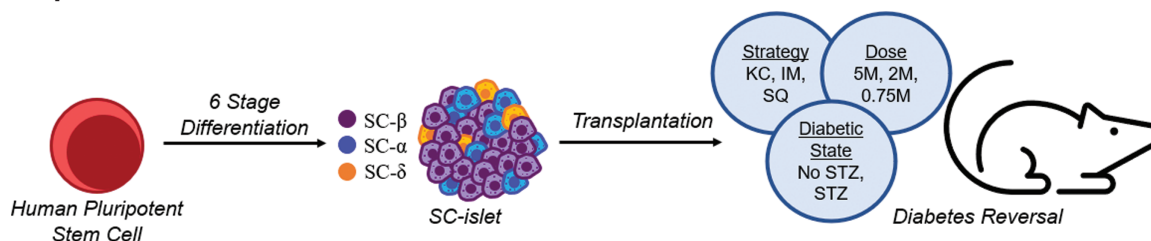
\*Corresponding author: Jeffrey R. Millman, Washington University School of Medicine, Southwest Tower 8th Floor, MSC 8127-057-08, 660 Euclid Avenue, St. Louis, MO 63110, USA. Tel: +1 (314) 362-3268; Fax: (314) 362-7641; Email: [jmillman@wustl.edu](mailto:jmillman@wustl.edu)

## Abstract

Insulin-producing stem cell-derived islets (SC-islets) provide a virtually unlimited cell source for diabetes cell replacement therapy. While SC-islets are less functional when first differentiated *in vitro* compared to isolated cadaveric islets, transplantation into mice has been shown to increase their maturation. To understand the effects of transplantation on maturation and function of SC-islets, we examined the effects of cell dose, transplantation strategy, and diabetic state in immunocompromised mice. Transplantation of 2 and 5, but not 0.75 million SC-islet cells underneath the kidney capsule successfully reversed diabetes in mice with pre-existing diabetes. SQ and intramuscular injections failed to reverse diabetes at all doses and had undetectable expression of maturation markers, such as MAFA and FAM159B. Furthermore, SC-islets had similar function and maturation marker expression regardless of diabetic state. Our results illustrate that transplantation parameters are linked to SC-islet function and maturation, providing ideal mouse models for preclinical diabetes SC therapy research.

**Key words:** stem cells; tissue-based therapy; diabetes mellitus; cell transplantation; insulin-secreting cells.

## Graphical Abstract



## Introduction

Diabetes is a metabolic disorder resulting from the death and dysfunction of insulin-producing  $\beta$  cells found within pancreatic islets. Cell replacement therapy is a potential treatment for patients with diabetes. Human pluripotent stem cell-derived islets (SC-islets) that transcriptionally and functionally resemble primary human islets are a potential renewable source of replacement cells.<sup>1–4</sup> Recent advances have enabled differentiation of SC-islets with high endocrine purity, including hormone-secreting  $\beta$ ,  $\alpha$ , and  $\delta$  cells, that undergo glucose-stimulated insulin secretion (GSIS) and successfully treat or prevent diabetes in mice.<sup>5–9</sup> This technology has facilitated the study of patient-derived SC-islets with diabetes, and explored employment of gene-editing strategies to reverse diabetes-causing gene variants. In addition, SC-islets have expanded the understanding of islet cell maturation molecular controls and differentiation *in vitro*.<sup>10–16</sup>

Despite these advances, SC-islets, particularly the  $\beta$  cells, are still immature when compared to isolated cadaveric islets both in terms of function and marker expression *in vitro*. Maturation has been described to occur after transplantation in mice in terms of function and marker expression.<sup>17–19</sup> Both non-diabetic mice and mice with pre-existing diabetes are used in studies.<sup>5,6,10–12,14,17,18,20–24</sup> Transplanting cells into nondiabetic mice prevents subsequent induction of diabetes, such as by streptozotocin (STZ) injection, but does not establish their ability to reverse it. The reported cellular doses transplanted vary widely in reports.<sup>12,17,18,20,23,25–27</sup> Location also varies, with common transplantation strategies including the SQ,<sup>22</sup> intramuscular (IM),<sup>14</sup> epididymal or mammary fat pad,<sup>27</sup> and kidney capsule (KC) locations.<sup>5,11,17,28</sup> The effects of dose, location, and diabetic state on function and maturation of SC-islets are unknown but relevant for clinical translation. Furthermore, a careful, controlled comparison of these important parameters has not been performed for SC-islets.

Received: 22 February 2021; Accepted: 17 October 2021.

© The Author(s) 2022. Published by Oxford University Press.

This is an Open Access article distributed under the terms of the Creative Commons Attribution-NonCommercial License (<https://creativecommons.org/licenses/by-nc/4.0/>), which permits non-commercial re-use, distribution, and reproduction in any medium, provided the original work is properly cited. For commercial re-use, please contact [journals.permissions@oup.com](mailto:journals.permissions@oup.com).

Here, we report the effects of dose, location, and diabetic state on transplanted SC-islets in immune-compromised mice. SC-islets were differentiated *in vitro* using a 6-stage differentiation protocol<sup>5</sup> and transplanted animals were monitored for up to 22 weeks. Transplantation with as few as 2 million cells underneath the KC reversed pre-existing STZ-induced diabetes while 0.75 million cells were insufficient. However, the recipient mice with pre-existing diabetes did not affect neither human C-Peptide levels in the serum nor maturation marker expression of the transplanted SC-islets. Other locations failed to both reverse diabetes and express maturation markers.

## Materials and Methods

### Cell Culture and Differentiation

Undifferentiated HUES8 human embryonic stem cells (hESCs) were graciously provided by Dr. Douglas Melton (Harvard University), were cultured in mTeSR1 (STEMCELL Technologies; 05850) on tissue culture plastic in a humidified 5% CO<sub>2</sub> 37°C tissue culture incubator. Every 3-4 days, SCs were passaged by single-cell dispersion using TrypLE (Life Technologies; 12-604-039), counted with Vi-Cell XR (Beckman Coulter), and seeded  $0.52 \times 10^6$  cells/cm<sup>2</sup> in mTeSR1 + 10 mM Y27632 (Abcam; ab120129) on Matrigel-coated (Corning; 356230) plates. To initiate differentiation, undifferentiated SCs were seeded at  $5 \times 10^6$  cells per well in a Matrigel-coated 6-well plate. Subsequent feeding schedules, media formulations, and differentiation factors are provided in [Supplementary Tables S1 and S2](#). On day 7 of stage 6, cells are single-cell dispersed using TrypLE and seeded at  $5 \times 10^6$  cells per well with 4 mL of stage 6 into a 6-well plate. The cells are cultured on an orbi-shaker (Benchmark) rotating at 100 RPM in a humidified 5% CO<sub>2</sub> 37°C tissue culture incubator. Brightfield images are taken throughout differentiation with a Leica DMI1.

### Immunostaining

SC-islets or transplanted cell extractions were fixed with 4% paraformaldehyde (Electron Microscopy Science; 15714) overnight at 4°C. SC-islet clusters were placed in Histogel (Thermo Fisher Scientific; Hg-4000-012) and transplant extractions were cut in half and processed by the Division of Comparative Medicine (DCM) Research Animal Diagnostic Laboratory Core at Washington University and Histowiz. Paraffin was removed with Histoclear (Electron Microscopy Sciences; 64111-04) and ethanol (Decon; 2716), samples were rehydrated, and antigens were retrieved in a pressure cooker (Proteogenix; 2100 Retriever) with 0.05M EDTA (Ambion; AM9261). Samples were blocked and primary antibodies were diluted in immunostaining buffer (5% Donkey Serum [Jackson ImmunoResearch; 017-000-121]) and 0.1% Triton-X (Acros Organics; 327371000) in phosphate-buffered saline (PBS) (Corning; 21-040-CV) and applied to samples overnight at 4°C in a humidified box. Next, secondary antibodies diluted in immunostaining buffer were added for 2 h at room temperature (RT), and then samples were mounted with DAPI Fluoromount-G (SouthernBiotech; 0100-20). Cells were imaged with a Leica DMI4000 fluorescence or Nikon A1Rsi confocal microscope. Images were processed with ImageJ. Flow cytometry was performed on single-cell dispersed SC-islets with TrypLE, fixed at RT for 30 minutes, and stained as described above. Cells were analyzed with BD LSR

Fortessa X-20 (BD Biosciences). FlowJo software generated population percentages and dot plots. Antibody details and dilutions are available in [Supplementary Table S3](#).

### Glucose-Stimulated Insulin Secretion

SC-islets were washed with Krebs-Ringer Bicarbonate (KRB) buffer (128 mM NaCl, 5 mM KCl, 2.7 mM CaCl<sub>2</sub>, 1.2 mM MgSO<sub>4</sub>, 1 mM Na<sub>2</sub>HPO<sub>4</sub>, 1.2 mM KH<sub>2</sub>PO<sub>4</sub>, 5 mM NaHCO<sub>3</sub>, 10 mM HEPES [Gibco; 15630-080], and 0.1% bovine serum albumin [BSA]) and transferred to transwells in 2 mM glucose KRB solution for 1 h to equilibrate. The solution was replaced with 2 mM glucose KRB for an additional 1 h and supernatant was collected. Last, solution was replaced with 20 mM glucose KRB for the final 1 h and supernatant was collected. Transwells were transferred to TrypLE for single-cell dispersion, incubated for 30 minutes, and counted with Vi-Cell XR to normalize insulin secretion. Insulin in supernatant was quantified with human insulin ELISA (ALPCO; 80-INSHU-E10.1). For all incubations, cells were placed in a humidified incubator at 37°C with 5% CO<sub>2</sub>.

### Transplantation Studies

All transplantation studies adhered to Institutional Animal Care and Use Committee regulations. All studies and surgeries were performed by unblinded individuals and mice were randomly assigned to experimental groups. Seven-week-old male NOD.Cg-Prkd<sup>scid</sup> Il2rg<sup>tm1Wjl/SzJ</sup> (NSG) mice were ordered from Jackson Laboratories (005557). Mice were rendered diabetic (blood glucose >500 mg/dL) with 5 consecutive days of 45 mg/kg STZ (R&D systems; 1621400) injections. Diabetic and nondiabetic mice were anesthetized and injected with a designated number of SC-islet cells in clusters according to their experimental group—(dose)  $5 \times 10^6$ ,  $2 \times 10^6$ , or  $0.75 \times 10^6$  into the KC of diabetic mice; (strategy)  $5 \times 10^6$  into the KC, IM, SQ, or intraperitoneal of diabetic mice; (diabetic state)  $5 \times 10^6$  into the KC of diabetic and nondiabetic mice. Sham diabetic and nondiabetic mice were used as controls. Sample size was not determined using a power calculation. KC transplants were performed with a 25G butterfly needle (TERUMO; SV\*25BLK). Cells transplanted in the IM, SC, or IP locations were injected with ~50 µL of Matrigel using a 27G needle (BD; 309623). For IM, cells were transplanted into the left thigh muscles. For SC, cells were transplanted on the left side of the back at the midline. SC-islet cells were produced from the same batch of differentiation to avoid potential confounding influence of batch-to-batch variation in the quality of the cells.

Blood glucose was measured with Contour NEXT Blood Glucose Monitoring System (Bayer). Random insulin serum was quantified throughout the study by tail bleed collection into microvettes (16.443.100, Sarstedt). Whole blood was centrifuged for 15 minutes at 2500 rpm at 4°C, serum was collected and stored at -80°C. Random weight measurements were taken on a scale (Adam Equipment; AE9CQ15186). Functional assessments included glucose tolerance test (GTT) and *in vivo* GSIS. For both assessments, mice were fasted for 4 h and injected with 2 g/kg glucose in 0.9% saline (MOLTOX; 51-405022.052). For GTT, blood glucose was measured every 30 minutes for 120 minutes. For *in vivo* GSIS, blood was collected using microvettes before and 1 h after glucose stimulation, centrifuged, and serum supernatant was transferred for storage at -80°C. Serum hormones were quantified with Mouse C-Peptide ELISA (ALPCO



Diagnostics; 80-CPTMS-E01), Human Ultrasensitive C-Peptide ELISA (Mercodia; 10-1141-01), Human Proinsulin ELISA, and Human Ultrasensitive Insulin ELISA (ALPCO Diagnostics; 80-ENSHUU-E01.1). Random mouse serum was collected in the AM (7:00-11:00) and GTT was performed in the PM (12:00-16:00). Nephrectomy was performed on mice with reversed diabetes by removing kidney with transplanted SC-islets. The blood glucose, weight, in vivo GSIS, random C-Peptide, and GTT data for the STZ, 5M KC mouse (royal blue) condition and diabetic controls (STZ, No Txp, gray) were repeatedly used in Figs. 2-4 and Supplementary Fig. S2 for multiple different transplantation methodology comparisons.

### Immunostaining Quantification

Sectioned slides were stained with islet (C-Peptide, Glucagon [GCG], Somatostatin), maturation markers (MAF BZIP transcription factor A [MAFA] and FAM159B), and DAPI as described above. For FAM159B, GCG, somatostatin, and C-Peptide, at least 3 representative images were taken for each transplant condition from up to 4 mice, starting at 14-week post-transplant. For MAFA, at least 3 representative images were taken for each transplant condition for 1 mouse at 14 wk post-transplant, as the supply of antibody for this study was limited. The number of cells per sectioned transplant ranged from 50-400 total cells, depending on the transplant condition and view of graft. For islet markers, the number of monohormonal (eg, C-Peptide+GCG- or C-Peptide-GCG+) and total number of grafted cells were counted. The ratio of specific islet cell types to the total cell number was calculated as a percentage. For maturation markers, the number of C-Peptide+ (green), and C-Peptide+MAFA+ or C-Peptide+FAM159B+ (green and red) cells were counted. The ratio of C-Peptide+MAFA+ or C-Peptide+FAM159B+ to C-Peptide+ was calculated as a percentage.

### Statistical Analysis

Statistical analysis was performed with GraphPad Prism 8.2.1. Two-sided unpaired and paired *t*-tests and one-way analysis of variance with Dunnett's or Tukey's multiple comparison test were performed when appropriate. Statistical tests are detailed in figure legends with sample size, *n*, indicating a total number of biological replicates. Data are shown as mean  $\pm$  SEM. *P* < .05 was considered statistically significant.

## Results

### In Vitro Differentiation of SC-Islets Before Transplantation

hESCs were differentiated into SC-islets with a recent differentiation protocol (Fig. 1A).<sup>5</sup> The SC-islets resembled primary human islet morphology, composition, and function (Fig. 1B and E).<sup>5,6,10,29</sup> This differentiation protocol produced almost exclusively endocrine (CHGA+) cells (93  $\pm$  3%) (Fig. 1D). SC- $\beta$  cells were the most prominent cell type generated in SC-islets, defined by C-Peptide+NKX6.1+ cells, which is consistent in multiple differentiations and when sampling multiple clusters (42  $\pm$  6%) (Fig. 1C and D). SC-islets were able to undergo GSIS, secreting more insulin in response to glucose (*P* = .0011, 2 mM, 487  $\pm$  71, 20 mM, 1655  $\pm$  216  $\mu$ U/10<sup>6</sup> cells) (Fig. 1E).<sup>6,10</sup>

SC-islets were transplanted to investigate the impact of multiple strategies (KC, IM, SQ), doses (5, 2, 0.75 million), and diabetic state (STZ and no STZ control) on maturation and function (Fig. 1F and 1G, Supplementary Fig. S1A). SC-islet transplant conditions were all performed in 8- to 10-week-old NSG immunodeficient mice from Jackson Laboratories. We used low-dose STZ injections over 5 days to render diabetes in the NSG mice. STZ-induced diabetic mice with sham transplants were established as controls throughout the study. Several mice with low amounts of circulating human insulin and all the STZ-induced diabetic mice were sacrificed at week 14 due to health concerns. The remaining mice were studied for 22 weeks to investigate the maturation, function, and ability to return blood glucose levels to euglycemia.

### KC Transplantation Reversed Diabetes in Mice

For this study, we transplanted 5 million SC-islet cells into mice at various locations including KC, IM, and SQ (Fig. 1G). Weekly fasting blood glucose measurements revealed KC transplants (blue) as the only location to reverse diabetes at 6 weeks post-transplantation (Fig. 2A). The SQ (green) and IM (orange) transplanted mice remained hyperglycemic with the lowest fasted weekly blood glucose measurement observed as 355  $\pm$  19 mg/dL at week 14 and 340  $\pm$  32 mg/dL at week 3, respectively. Interestingly, the IM strategy showcased high and low blood glucose spikes from weeks 1 to 12 until the values plateaued averaging 578  $\pm$  14 mg/dL from week 12 onward (Fig. 2A). Furthermore, the SQ location, averaging blood glucose 458  $\pm$  40 mg/dL over 22 weeks, had some reduction in blood glucose, maintaining less severe hyperglycemia than the IM transplants from week 3 until the conclusion of the study (Fig. 2A). Vascularization and SC-islet grafts were visible in all explanted strategy sites at 14- and 22-weeks post-transplantation (Fig. 1G, Supplementary Fig. S1A and B). Furthermore, weight remained similar between transplanted mice however, the diabetic no transplant (gray) mice weighed less beginning at week 2 compared to all transplanted groups (*P* = .02) (Supplementary Fig. S2A).

We collected random mouse serum, and quantified human C-Peptide measurements which indicated less C-Peptide secretion in IM and SQ transplants compared to the KC (Fig. 2B). We performed a GTT and in vivo GSIS to determine glucose tolerance and glucose-responsive insulin secretion, respectively. We conducted the assays after 4 h fasts with an intraperitoneal injection of 2 mg/kg glucose. Remarkably, all strategies contained functional SC-islets at 6 weeks post-transplantation yielding a stimulation index greater than 1.0 (KC, 3.6  $\pm$  0.9; IM, 10.2  $\pm$  5.6; SQ, 1.9  $\pm$  0.7; *P* = .21) (Fig. 2C). However, the SQ and IM strategies had lower insulin secretion at both low and high glucose compared to the KC transplants (Fig. 2C). A high functioning graft requires both high concentrations of C-Peptide and an in vivo stimulation index, which is only identified in the KC transplant. This is further supported by weekly blood glucose monitoring and random C-Peptide values. The only glucose tolerant mice at 6 weeks post-transplantation contained the KC transplant, whereas the IM and SQ strategies remained hyperglycemic throughout the 120 minutes assay (Fig. 2D).

At least one animal per condition was sacrificed at week 14 to determine composition and maturation of the sectioned grafts. Up to 3 additional animal grafts were collected up to week 22 for histological analysis. For all locations, C-Peptide expressing SC- $\beta$  cells were present as well as GCG+ SC- $\alpha$  and

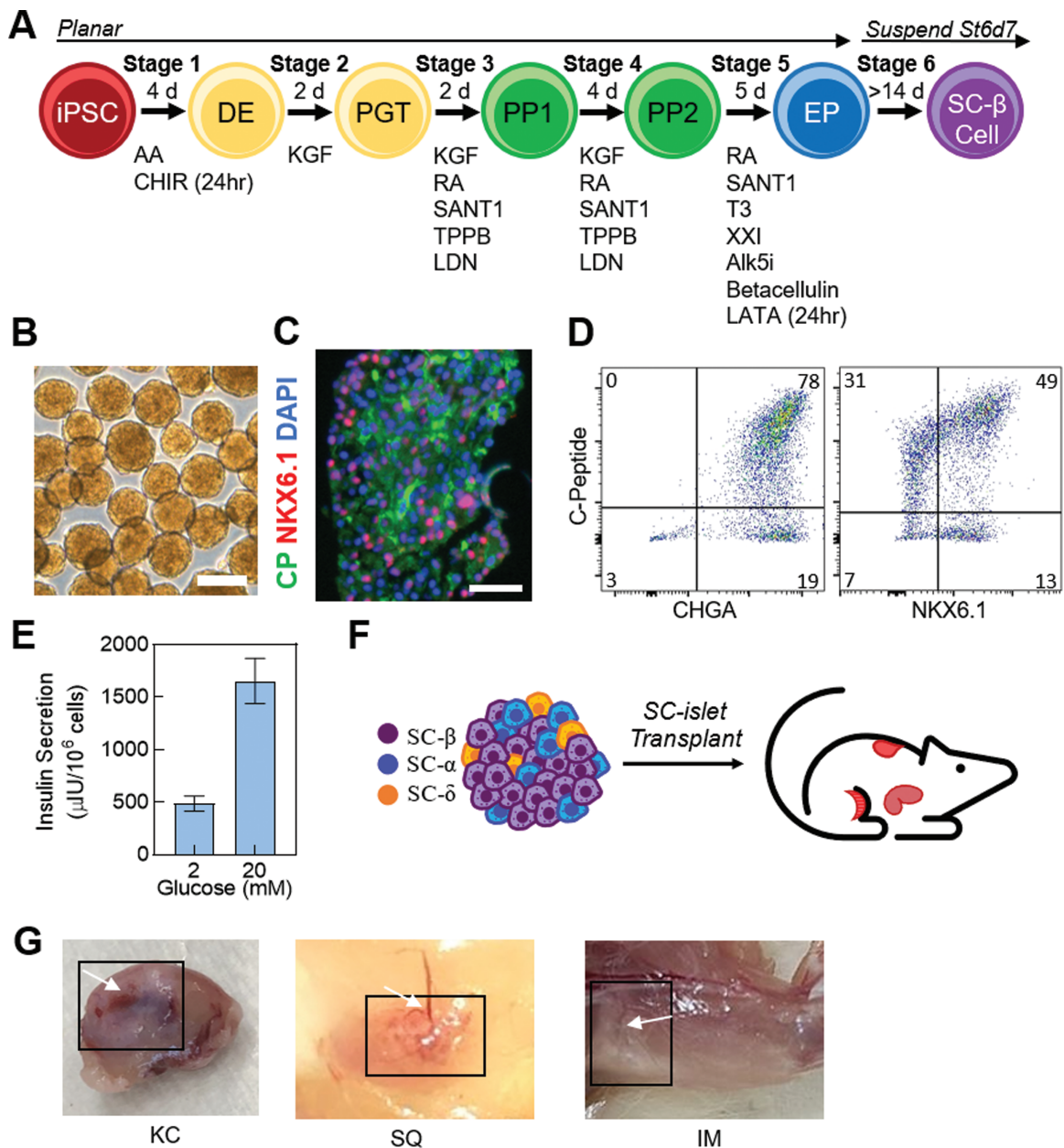


**Figure 1.** Characterization of stem cell-derived islets (SC-islets) in vitro. **(A)** Schematic of 6-stage differentiation protocol to generate SC-islets. **(B)** Brightfield images of stage 6 SC-islets generated in vitro. Scale bar = 250 μm. **(C)** Immunostained sections and **(D)** representative flow cytometry plots of stage 6 SC-islets for islet and β cell markers. Scale bar = 50 μm. **(E)** Static GSIS of SC-islets in vitro ( $n = 4$ , replicates transplanted in mice). **(F)** Schematic of different transplantations assessed in the study. **(G)** Images of explanted grafts in kidney capsule (KC), subcutaneous (SQ), and intramuscular (IM) locations. Black boxes frame graft and white arrows point to blood vessel formation. Results are mean ± SEM. CP, C-Peptide, green; NKX6.1, red; DAPI, DAPI, 4',6-diamidino-2-Phenylindole, blue.

somatostatin+ SC-δ cells (Fig. 2E, Supplementary Fig. S2B and C). For the IM transplants, fewer C-Peptide+ SC-β and GCG+ SC-α cells were present and the GCG protein presence was weak compared to the mice implanted in the KC (Supplementary Fig. S2B). We immunostained FAM159B and MAFA, both of which are maturation markers for β cells and associated with post-transplantation maturation for SC-β cells,<sup>30,31</sup> to determine maturation of the SC-islets in vivo. They were also specific to pancreatic endocrine, distinguishing cells from exocrine<sup>32</sup> which were present in the grafts, as previously reported,<sup>5</sup> but not in stage 6 SC-islets in vitro (Supplementary Fig. S2D). FAM159B encodes a membrane protein that

regulates exocytosis therefore the FAM159B+C-Peptide- cells may be identified as other endocrine hormone-secreting cell types (Fig. 2E and Supplementary Fig. S2B). Several C-Peptide cells coexpressed FAM159B in the KC graft indicating maturation of the SC-β cells (Fig. 2E, Supplementary Fig. S2B and C). The IM location had no FAM159B expression and surprisingly, the SQ graft had several FAM159B+ cells, however, few were coexpressed with C-Peptide (Figs. 2E, Supplementary Fig. S2B and C). MAFA is a well-known maturation marker for β cells<sup>5,17,31,33</sup> and is present in a high percentage of C-Peptide+ SC-β cells when transplanted in the KC<sup>31</sup> ( $59 \pm 4\%$ , Fig. 2E and Supplementary Fig. S2E). Alternatively, the IM and SQ



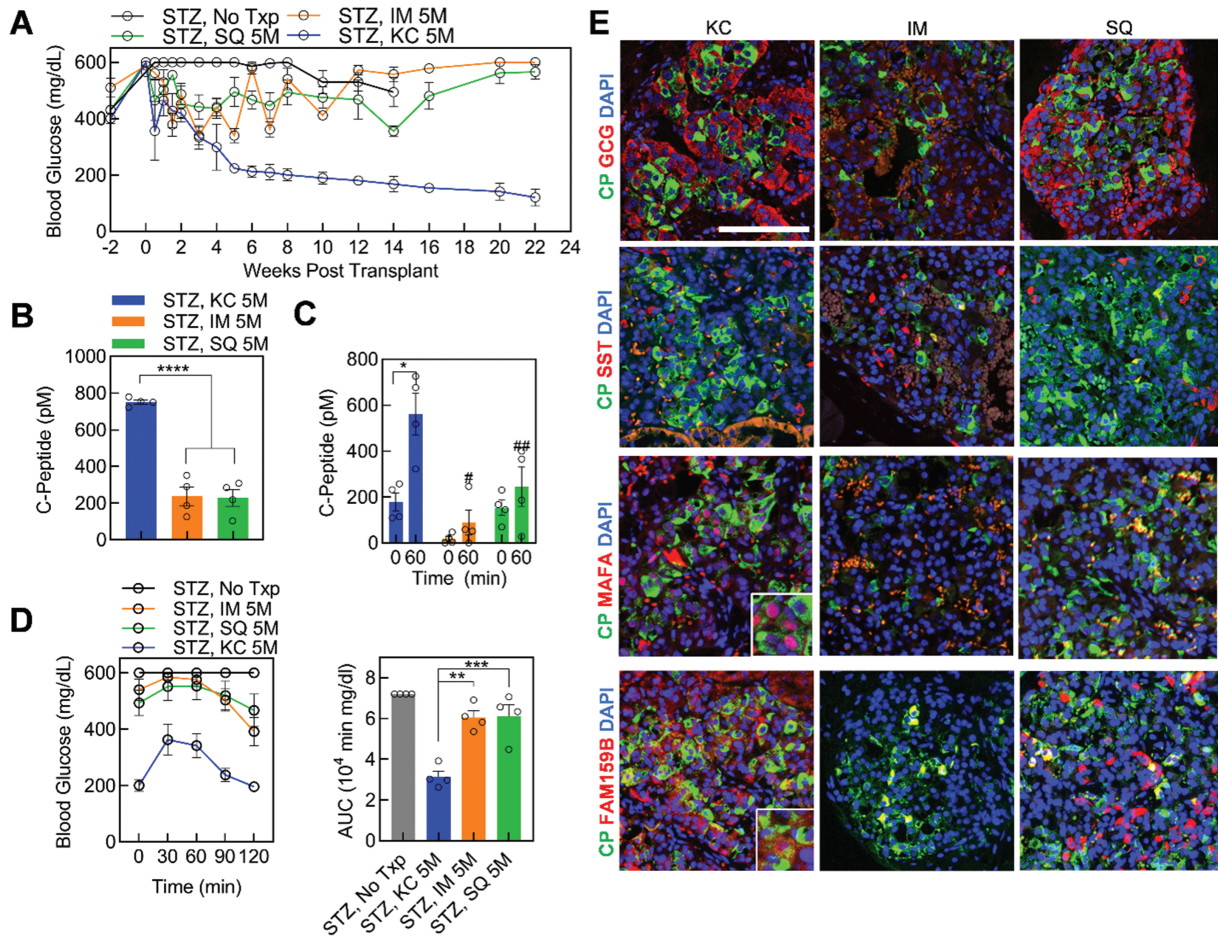


**Figure 2.** Transplantation of stem cell-derived islets (SC-islets) in diabetic mice using multiple strategies. **(A)** Blood glucose before and after STZ treatment and transplantation of 5 million SC-islet cells into the kidney capsule (KC; streptozotocin [STZ], KC 5M; blue,  $n = 4$ ), subcutaneous space (STZ, SQ 5M; green,  $n = 4$ ), or in the muscle (STZ, IM 5M; orange,  $n = 4$ ), and diabetic (STZ, No Txp; dark gray,  $n = 4$ ) controls ( $n = 4$ ). **(B)** Random serum human C-Peptide measurement in all transplant sites ( $n = 4$ ) at 2 weeks post-transplantation. \*\*\*\* $P < .0001$  by 2-way unpaired  $t$ -test. **(C)** In vivo GSIS at 6 weeks post-transplantation for all transplant strategies in diabetic mice at 0 and 60 minutes following 2 g/kg intraperitoneal glucose injection ( $n = 4$ ). \* $P < .05$  by 2-way paired  $t$ -test comparing 0- and 60-minutes time points. # $P < .05$ , ## $P < .01$  by 2-way unpaired  $t$ -test comparing 60 minutes timepoint from IM and SQ to KC. **(D)** Glucose tolerance test (GTT) blood glucose and area under the curve (AUC) quantification at 6 weeks after transplant ( $n = 4$ ). \*\* $P < .01$ , \*\*\* $P < .001$  by 2-way unpaired  $t$ -test compared between transplantation strategies. **(E)** Representative images of immunostained sectioned graft explanted from each mouse transplantation location at 14 weeks post-transplantation for islet and beta-cell maturation markers. Scale bar = 100  $\mu\text{m}$ . SST, somatostatin. See also [Supplementary Fig. S2](#). Results are mean  $\pm$  SEM.

grafts contained no MAFA+C-Peptide+ cells (SC,  $0 \pm 0\%$ , IM,  $0 \pm 0\%$ ), implying a lack of maturation with these strategies (Fig. 2E and [Supplementary Fig. S2E](#)). Furthermore, we immunostained grafted and in vitro SC-islets with MAFB following transplantation ([Supplementary Fig. S2F](#)). In summary, the KC transplantation location was more advantageous compared to IM and SQ when assessing SC-islet cell therapy due to its ability to reverse diabetes in mice and mature SC-islets in vivo.

### A Dose of 5 and 2 Million SC-Islet Cells reversed Diabetes in Mice

In previous reports, we transplanted 5 million cells into the KC.<sup>5,6,10</sup> To determine if fewer cells could produce similar results, we reduced the number of transplanted cells in this study, surveying the cell therapy potential of 5 (dark blue), 2 (medium blue), and 0.75 (light blue) million SC-islet cells transplanted into the KC of mice with pre-existing diabetes. Weekly blood glucose measurements revealed the reversal of diabetes in mice with 5 and 2 million transplanted SC-islet

cells (Fig. 3A and B). Alternatively, the 0.75 million SC-islet transplants failed to reverse diabetes throughout the 22-week study, with mice remaining severely hyperglycemic and displaying significant weight loss ( $28 \pm 1$  g, week 7) beginning at week 7 until the completion of the study, relative to the 2 ( $30.5 \pm 0.6$  g, week 7,  $P = .045$ ) and 5 ( $31.2 \pm 0.8$  g, week 7,  $P = .016$ ) million SC-islet transplanted mice (Fig. 3A and B, [Supplementary Fig. S3A](#)).

Circulating human C-Peptide in the mouse serum 2 weeks post-transplant was greater in the 2 and 5 million SC-islet doses compared to the 0.75 million SC-islet transplanted mice (Fig. 3C). At 6 weeks post-transplantation, 2 and 5 million SC-islet transplanted mice attained euglycemia and in vivo GSIS displayed glucose-responsive C-Peptide secretion for the nondiabetic transplanted mice (Fig. 3D). Furthermore, the mice transplanted with 2 and 5 million cells had indistinguishable glucose tolerance indicated by GTT at week 6 (Fig. 3E), whereas the 0.75 million SC-islet transplanted mice had dysfunctional, low insulin-secreting cells lacking glucose tolerance with a GTT profile similar to

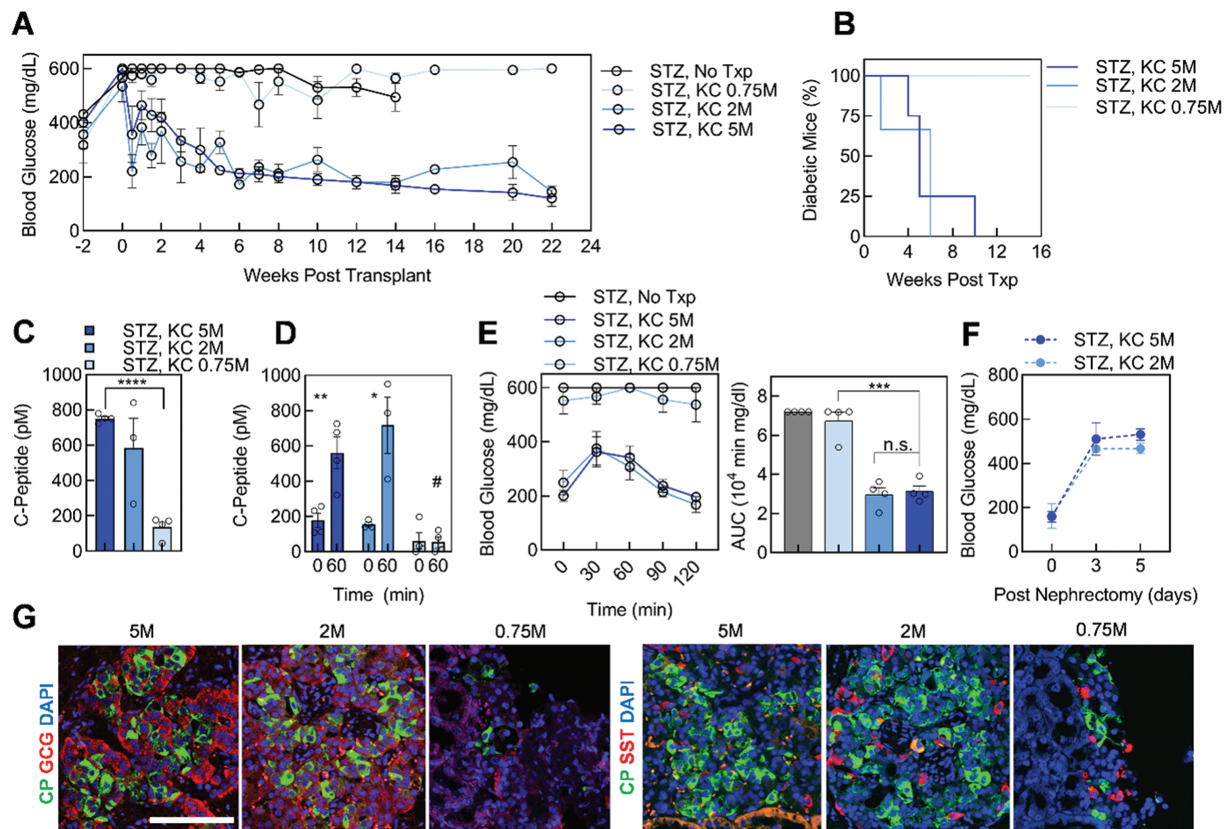


**Figure 3.** Various stem cell-derived islet (SC-islet) doses transplanted into the kidney capsule of diabetic mice. **(A)** Blood glucose measurements before and after streptozotocin (STZ) treatment and kidney capsule (KC) transplantation of either 5 (STZ, KC 5M; dark blue;  $n = 4$ ), 2 (STZ, KC 2M; medium blue;  $n = 3$ ), or 0.75 (STZ, KC 0.75M; light blue;  $n = 4$ ) million SC-islet cells, and diabetic (STZ, No Txp; dark gray;  $n = 4$ ) controls. **(B)** Diabetes reversal curve for each transplant condition (STZ, KC 2M,  $n = 3$ ; STZ, KC 5M and STZ, KC 0.75M  $n = 4$ ). **(C)** Human C-Peptide quantification for random serum collection from transplanted mice at 2 weeks post-transplantation (STZ, KC 2M,  $n = 3$ ; STZ, KC 5M and STZ, KC 0.75M  $n = 4$ ). \*\*\*\*  $P < .0001$  by 2-way unpaired  $t$ -test. **(D)** In vivo GSIS of transplanted mice (STZ, KC 2M,  $n = 3$ ; STZ, KC 5M and STZ, KC 0.75M  $n = 4$ ). \* $P < .05$ , \*\* $P < .01$  by 2-way paired  $t$ -test comparing 0- and 60-minutes time points. # $P < .05$ , by 2-way unpaired  $t$ -test comparing 60 minutes between doses. **(E)** Glucose tolerance test (GTT) blood glucose measurements and area under the curve (AUC) quantification for transplanted and diabetic mice (STZ, KC 2M,  $n = 3$ ; all other conditions,  $n = 4$ ). \*\*\* $P < .001$ , n.s., not significant, by 2-way unpaired  $t$ -test comparing transplant conditions. **(F)** Blood glucose measurements after nephrectomy of 2 STZ, KC 2M and 3 STZ, KC 5M mice. **(G)** Sectioned grafts were explanted and immunostained for all doses at 14 weeks post-transplantation with DAPI (blue) and islet markers. Images are representative of a single graft per dose. Scale bar = 100  $\mu\text{m}$ . See also [Supplementary Fig. S2](#). Results are mean  $\pm$  SEM.

the diabetic controls (gray) (Fig. 3E). We performed nephrectomy on two 2 million and three 5 million SC-islet transplanted mice following diabetes reversal and observed a return to hyperglycemia 3 days following the nephrectomy in all mice (Fig. 3F).

Excised grafts from at least one mouse per dose after 14 weeks in vivo, and up to 3 mice at 22 weeks in vivo, further emphasized the similarity between 5 and 2 million SC-islet transplanted mice (Fig. 3G, [Supplementary Fig. S3B and C](#)). In both conditions, C-Peptide, GCG, and somatostatin positive cells indicated the presence of 3 major endocrine cell types in vitro post engraftment (Fig. 3G, [Supplementary Fig. S3B and C](#)). The 0.75 million cell transplanted graft had a smaller width for cell detection, as seen in the grafted kidney (Fig. 1B and [Supplementary Fig. S1A](#)), containing fewer C-Peptide expressing SC- $\beta$  cells compared to a dose of 5 million cells ([Supplementary Fig. S3B](#)). In contrast, a similar proportion of somatostatin expressing SC- $\delta$  and GCG expressing SC- $\alpha$  cells remained ([Supplementary Fig. S3B](#)). Together, these results indicated 2 million SC-islet cells generated with our differentiation protocol provided a similar therapeutic effect as 5 million transplanted cells.

### The Diabetic Environment at SC-Islet Transplantation Did Not Affect Maturation

To continue evaluating different mouse models, we determined the effect of a diabetic environment on SC-islet function and maturation in vivo. We transplanted 5 million SC-islet cells into the KC of STZ-induced diabetic and nondiabetic mice. Mice transplanted with cells gained weight at a similar rate to healthy, nondiabetic control mice ([Supplementary Fig. S3D](#)). Weekly blood glucose measurements displayed a return to euglycemia for the STZ-treated transplants at 6 weeks and similar blood glucose levels between the STZ-treated and nondiabetic transplanted mice at 16 weeks (Fig. 4A). C-Peptide measurements were similar between STZ-treated and nondiabetic mice (Fig. 4B and C). To evaluate potential stress on SC-islets transplanted into a diabetic environment, we quantified the human proinsulin/insulin ratio in mouse serum at 2 weeks post-transplantation. We detected a similar ratio for SC-islets in both mouse conditions (Fig. 4D), implying a hyperglycemic mouse environment did not affect insulin processing. Furthermore, the mice displayed similar glucose tolerance 6 weeks following SC-islet transplantation (Fig. 4E).



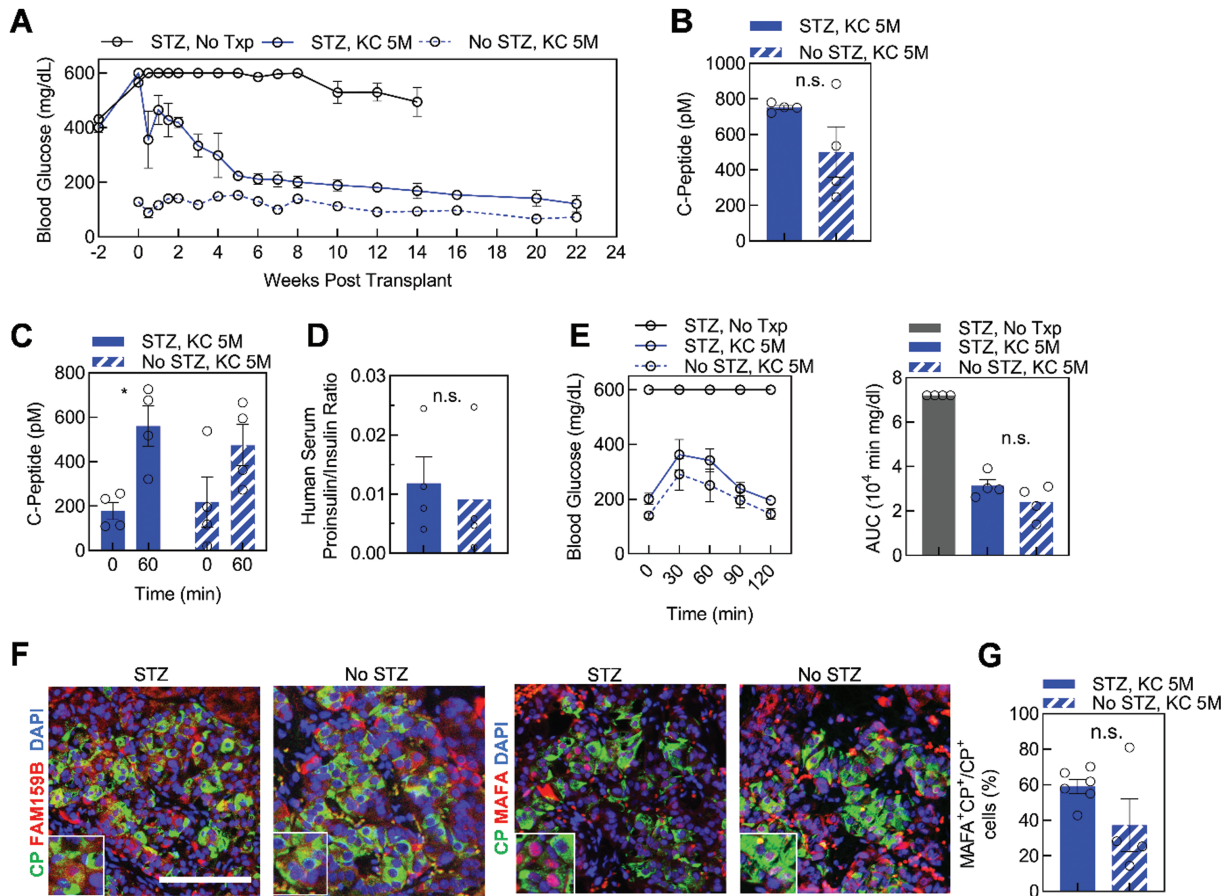


**Figure 4.** Diabetic environment effect on function and maturation of kidney capsule [KC] transplanted stem cell-derived islets (SC-islets). **(A)** Blood glucose measurements for streptozotocin (STZ)-treated diabetic (STZ, KC 5M, blue,  $n = 4$ ) and nondiabetic (No STZ, KC 5M, blue and white stripe,  $n = 4$ ) mice transplanted with 5 million SC-islet cells and diabetic (STZ, No Txp,  $n = 4$ ) control mice. **(B)** Random serum human C-Peptide collected from transplanted mice at 2 weeks post-transplantation ( $n = 4$ ). n.s., not significant by 2-way unpaired  $t$ -test. **(C)** In vivo GSIS of transplanted mice. Human C-Peptide is quantified before and 60 minutes after glucose injection at 6 weeks post-transplantation ( $n = 4$ ).  $*P < .05$  by 2-way paired  $t$ -test comparing 0 and 60 minutes. **(D)** Ratio of human proinsulin and insulin in mouse serum 2 weeks post-transplantation ( $n = 4$ ). n.s., not significant by 2-way unpaired  $t$ -test. **(E)** Glucose tolerance test (GTT) and area under the curve (AUC) quantification for all mouse conditions ( $n = 4$ ) 6 weeks following transplantation. n.s., not significant by 2-way unpaired  $t$ -test between transplant conditions. **(F)** Immunostaining of explanted KC grafts for DAPI (blue) and  $\beta$  cell maturation markers. Images are representative of SC-islets within a single graft for each condition. Scale bar = 100  $\mu$ m. **(G)** Quantification of MAFA<sup>+</sup>C-Peptide<sup>+</sup> cells from total C-Peptide<sup>+</sup> cells for multiple SC-islets within a single graft presented as transplanted diabetic (STZ, KC 5M,  $n = 8$ ) and nondiabetic (No STZ, KC 5M,  $n = 4$ ) mice. n.s., not significant by 2-way unpaired  $t$ -test. See also [Supplementary Fig. S2](#). Results are mean  $\pm$  SEM.

Grafted kidneys from both transplant conditions explanted at week 14- and 22-weeks post-transplantation contained a similar composition of endocrine cell types represented by C-Peptide, GCG, and somatostatin positive cells ([Supplementary Fig. S3E and F](#)). In both diabetic environments, the transplanted SC-islets had only monohormonal cells in the graft ([Supplementary Fig. S2F](#)). Both STZ and no STZ grafts had FAM159B and MAFA coexpression with C-Peptide<sup>+</sup> SC- $\beta$  cells, suggesting the diabetic environment is independent of in vivo maturation ([Fig. 4F](#)). The percentage of MAFA<sup>+</sup> (STZ,  $59 \pm 4\%$ , No STZ,  $37 \pm 15\%$ ) and FAM159B+ SC- $\beta$  (C-Peptide<sup>+</sup>) cells was similar between SC-islet transplants into diabetic and nondiabetic mice ([Fig. 4F and G, Supplementary Fig. S3E](#)). In conclusion, transplanting high-functioning SC-islets into either STZ-induced diabetic or nondiabetic mice yielded similar results for maturation of the SC- $\beta$  cells, human insulin processing, and random C-Peptide secretion in the mouse serum.

## Discussion

Diabetes cell therapy using differentiated SCs will likely be one of the first, most widespread uses of cell replacement therapy technology. To translate diabetes cell therapy to the clinic, animal models are needed to test the efficacy of SC-islets. This controlled study evaluated several transplantation parameters in mice. Our generated results provide a greater understanding of maturation and function of SC-islets impacted by transplantation strategy, dose, and host diabetic state.

Research groups investigating the potential for SC-islets and related insulin-producing cell types for diabetes cell therapy have varied transplantation parameters. In this study, our transplantation strategies include SQ, IM, and KC sites. Technical expertise can influence strategy preference with IM surgeries having a high failure<sup>14</sup> and operative mortality rate,<sup>34</sup> while SQ transplants are a routine, easy to learn procedure. Of note, the KC is not a translatable location in human patients. However, it is an ideal location to observe maturation

and function of the SC-islets in mice due to its contained location and rapid vascularization.

In this study, we transplanted 0.75, 2, and 5 million SC-islet cells and demonstrated that lower cell numbers (2 million) than routinely used for mouse models<sup>5-7,17,19,35</sup> are sufficient. Specifically, previous studies required transplantation of larger cell doses ranging from approximately 1 to 20 million, derived from various differentiation protocols.<sup>12,17,18,20,23,25-27</sup> The numbers that we transplanted were chosen to span the spectrum of lower doses, as we had previously established that 5 million SC-islet cells were sufficient in the KC of mice<sup>5,10</sup> and we wanted to have a value lower than typical. Reduced differentiation efficiency would require larger doses. Our effective dose of 2 million cells in mice may be attributed to higher SC- $\beta$  cell fractional yields in the SC-islets and/or high function in vitro. Our results demonstrated 0.75 million SC-islet cells were unable to reach euglycemia following transplant. Further study into intermediate cell doses would be useful to better understand this parameter on achieving euglycemia.

In this study, we characterized the maturation of SC- $\beta$  cells through elevated C-peptide, a proxy marker for insulin, and an increased fraction of C-Peptide+/MAFA+ and C-Peptide+/FAM159B+  $\beta$  cells. There is heterogeneity of FAM159B in  $\beta$  cells, which remains unclear.<sup>30,36</sup> The impact of transplantation parameters on other islet endocrine cell function and maturation, such as SC- $\alpha$ , SC- $\delta$ , and SC-enterochromaffin cells, remains unclear. Furthermore, the cross-reactivity of antibodies, such as the MAFA antibody to MAFB, remains a possibility. Additional limitations of our study include the various unevaluated parameters. There are multiple chemicals that can induce diabetes including STZ and alloxan,<sup>12</sup> and each needs to be optimized due to variable sensitivity between rodent strains.<sup>37</sup> We used exclusively male mice in our experimental design given the well-documented difficulties with rendering female mice diabetic by STZ or alloxan.<sup>37,38</sup> Alternate primary or SC-islet transplantation strategy sites not evaluated in our study include the spleen, intraperitoneal space, omentum, and portal vein. Moreover, the study of the various transplantation parameters in a larger sample size would be favorable. Furthermore, there are multiple strains of rodents used in previous studies to evaluate diabetes cell therapy, including TCR $\alpha^{-/-}$ , B6-RAG $^{-/-}$ , nonobese diabetic-SCID, and SCID-beige mice transplanted with SC-PP2 cells,<sup>39</sup> and C57BL/6J mice and nude rats transplanted with SC-PP2 and SC- $\beta$  cells.<sup>20</sup> Rodents are not the most physiologically relevant animal model to evaluate some transplantation strategies which require larger animal models. Non-primates and large nonhuman primate models, specifically, are of great importance for preliminary clinical trial data. Additionally, we transplanted stage 6 terminally differentiated SC-islets while other groups have used pancreatic progenitors, which were previously compared.<sup>21</sup> Of note, progenitor-derived protocols and diseased SC- $\beta$  cells<sup>10</sup> can lead to overgrowths or tumor formation, which are not observed in our transplants. Currently, clinical trials aim to achieve insulin independence in patients with diabetes by transplanting SC-islets (NCT04786262)<sup>40</sup> or pancreatic progenitors (NCT04678557).<sup>41</sup>

Several other groups are also working to move the field forward for clinical translation of diabetes cell therapy. While transplantation into the mouse KC has been optimized by many groups for many years,<sup>42,43</sup> it is not translatable to humans. Therefore, groups continue efforts to improve the IM and SQ locations, which may require larger SC-islet doses

or an alternative delivery approach than used here to rescue diabetes. Encapsulation devices are being tested to protect transplanted cells from the immune system and increase vascularization upon transplantation.<sup>22,27,44</sup> A recent report has shown that a collagen hydrogel formulation can improve islet efficacy upon transplantation subcutaneously.<sup>45</sup> Ongoing clinical trials use immunoprotective encapsulation devices transplanted in the SQ space (NCT04678557, NCT03513939).<sup>41,46</sup> Advancements in biocompatible materials for encapsulation devices are also progressing to create sturdy (polytetrafluoroethylene),<sup>47-49</sup> durable (polycaprolactone),<sup>50,51</sup> and retrievable (thread-reinforced alginate fibers)<sup>52</sup> devices for islet encapsulation targeting transplantation in the SQ space. Recent advances in device fabrication demonstrated a biocompatible, safe, and retrievable device using nanospinning with TSPU and an alginate core to transplant human SC-islets intraperitoneally in immunocompetent mice and dogs with minimal immune response.<sup>35</sup> Macro- and microencapsulation strategies<sup>8,44,53</sup> and immune cloaking through gene editing<sup>54,55</sup> are also being used to evade immunosuppression of transplanted SC-islets and primary human islets. In addition to protecting the transplanted cells, increasing the proportion of the SC- $\beta$  cell population within SC-islets or enhancing function of the SC- $\beta$  cells would render a lower therapeutic dose needed for transplantation in patients with diabetes. Several groups are working on strategies to generate a higher proportion of SC- $\beta$  cells by sorting pancreatic progenitor and  $\beta$  cells.<sup>7,9,33,56</sup> Combining advances in differentiation protocols, encapsulation methods, sorting for purified cell populations, and gene editing to evade the immune system will help generate a diabetes cell replacement therapy.

## Conclusion

Here, we demonstrate that common transplantation parameters affect the function and maturation of SC-islets in mice. As few as 2 million SC-islet cells reversed diabetes but 0.75 million cells were unable to achieve reversal. Transplantation in the KC resulted in higher serum C-peptide and better glycemic control compared to IM and SQ sites. In addition, serum C-peptide was similar between STZ-treated and nondiabetic mice. Expression of the maturation markers FAM159B and MAFA was only achieved by transplantation underneath the kidney capsule and was unaffected by the diabetic state of the animal.

## Acknowledgments

Equipment: Microscopy was performed at the WU Center for Cellular Imaging.

## Funding

Dr. Jeffrey R. Millman is the guarantor of this study and had full access to all data. He takes full responsibility for the integrity and data analysis of this study. This work was supported by Washington University (Departments of Surgery, Medicine, and Pediatrics), Mid-America Transplant Services, The Foundation for Barnes-Jewish Hospital, NIH (R01DK114233), JDRF Career Development Award (5-CDA-2017-391-A-N). Microscopy was supported by the Washington University Diabetes Research Center (P30DK020579).



## Conflict of Interest

Kristina G. Maxwell and Jeffrey R. Millman are Co-Founders of Salentra Biosciences. Jeffrey R. Millman is an inventor on patents and patent applications for material described in this manuscript and a consultant for Sana Biotechnology. The other authors declared no potential conflicts of interest.

## Author Contributions

K.G.M.: conception and design, collection and assembly of data, data analysis and interpretation, manuscript writing, final approval of the manuscript; M.H.K.: collection and assembly of data, final approval of the manuscript; S.E.G.: collection and assembly of data, final approval of the manuscript; J.R.M.: conception and design, financial support, collection and assembly of data, data analysis and interpretation, manuscript writing, final approval of the manuscript.

## Data Availability

We thank Dr. Kevin D'Amour (ViaCyte, Inc.) for the MAFA antibody. All data needed to evaluate the conclusions in the paper are present in the paper and/or the Supplementary materials. Additional data related to this paper may be requested from the authors.

## Supplementary Material

Supplementary material is available at *Stem Cells Translational Medicine* online.

## References

- Velazco-Cruz L, Goedegebuure MM, Millman JR. Advances toward engineering functionally mature human pluripotent stem cell-derived  $\beta$  cells. *Front Bioeng Biotechnol.* 2020;8:786.
- Aghazadeh Y, Nostro MC. Cell therapy for type 1 diabetes: current and future strategies. *Curr Diab Rep.* 2017;17(6):37.
- Tremmel DM, Mitchell SA, Sackett SD, et al. Mimicking nature-made beta cells: recent advances towards stem cell-derived islets. *Curr Opin Organ Transplant.* 2019;24(5):574-581.
- Domínguez-Bendala J, Inverardi L, Ricordi C. Stem cell-derived islet cells for transplantation. *Curr Opin Organ Transplant.* 2011;16(1):76-82.
- Hogrebe NJ, Augsornworawat P, Maxwell KG, et al. Targeting the cytoskeleton to direct pancreatic differentiation of human pluripotent stem cell. *Nat Biotechnol.* 2020;38(4):460-470.
- Velazco-Cruz L, Song J, Maxwell KG, et al. Acquisition of dynamic function in human stem cell-derived  $\beta$  cells. *Stem Cell Rep.* 2019;12(2):351-365.
- Nair GG, Liu JS, Russ HA, et al. Recapitulating endocrine cell clustering in culture promotes maturation of human stem-cell-derived  $\beta$  cells. *Nat Cell Biol.* 2019;21(2):263-274.
- Yoshihara E, O'Connor C, Gasser E, et al. Immune-evasive human islet-like organoids ameliorate diabetes. *Nature.* 2020;586:606-611.
- Mahaddalkar PU, Scheibner K, Pfluger S, et al. Generation of pancreatic  $\beta$  cells from CD177+ anterior definitive endoderm. *Nat Biotechnol.* 2020;38:1061-1072.
- Maxwell KG, Augsornworawat P, Velazco-Cruz L, et al. Gene-edited human stem cell-derived  $\beta$  cells from a patient with monogenic diabetes reverse preexisting diabetes in mice. *Sci Transl Med.* 2020;12(540):eaax9106
- Balboa D, Saarimäki-Vire J, Borshagovskiy D, et al. Insulin mutations impair beta-cell development in a patient-derived iPSC model of neonatal diabetes. *eLife.* 2018;7:e38519.
- Millman JR, Xie C, Van Dervort V, et al. Generation of stem cell-derived  $\beta$ -cells from patients with type 1 diabetes. *Nat Commun.* 2016;7:11463.
- Cardenas-Diaz FL, Osorio-Quintero C, Diaz-Miranda MA, et al. Modeling monogenic diabetes using human ESCs reveals developmental and metabolic deficiencies caused by mutations in HNF1A. *Cell Stem Cell.* 2019;25(2):273-289.e5. e275.
- Ma S, Viola R, Sui L, et al.  $\beta$  cell replacement after gene editing of a neonatal diabetes-causing mutation at the insulin locus. *Stem Cell Rep.* 2018;11(6):1407-1415.
- Leite NC, Sintov E, Meissner TB, et al. Modeling type 1 diabetes in vitro using human pluripotent stem cells. *Cell Rep.* 2020;32(2):107894.
- Russell R, Carnese PP, Hennings TG, et al. Loss of the transcription factor MAFB limits  $\beta$ -cell derivation from human PSCs. *Nat Commun.* 2020;11(1):1-15.
- Pagliuca FW, Millman JR, Gurtler M, et al. Generation of functional human pancreatic beta cells in vitro. *Cell.* 2014;159(2):428-439.
- Rezania A, Bruin JE, Arora P, et al. Reversal of diabetes with insulin-producing cells derived in vitro from human pluripotent stem cells. *Nat Biotechnol.* 2014;32(11):1121-1133.
- Augsornworawat P, Maxwell KG, Velazco-Cruz L, et al. Single-cell transcriptome profiling reveals  $\beta$  cell maturation in stem cell-derived islets after transplantation. *Cell Rep.* 2020;32(8):108067.
- Bruin JE, Asadi A, Fox JK, et al. Accelerated maturation of human stem cell-derived pancreatic progenitor cells into insulin-secreting cells in immunodeficient rats relative to mice. *Stem Cell Rep.* 2015;5(6):1081-1096.
- Bruin JE, Rezania A, Xu J, et al. Maturation and function of human embryonic stem cell-derived pancreatic progenitors in macroencapsulation devices following transplant into mice. *Diabetologia.* 2013;56(9):1987-1998.
- Pepper AR, Pawlick R, Bruni A, et al. Transplantation of human pancreatic endoderm cells reverses diabetes post transplantation in a prevascularized subcutaneous site. *Stem Cell Rep.* 2017;8(6):1689-1700.
- Saber N, Bruin JE, O'Dwyer S, et al. Sex differences in maturation of human embryonic stem cell-derived  $\beta$  cells in mice. *Endocrinology.* 2018;159(4):1827-1841.
- Shang L, Hua H, Foo K, et al.  $\beta$ -Cell dysfunction due to increased ER stress in a stem cell model of Wolfram syndrome. *Diabetes.* 2014;63(3):923-933.
- L S, Danzl N, Campbell SR, et al.  $\beta$ -Cell replacement in mice using human type 1 diabetes nuclear transfer embryonic stem cells. *Diabetes.* 2018;67(1):26-35.
- Nostro MC, Sarangi F, Yang C, et al. Efficient generation of NKX6-1+ pancreatic progenitors from multiple human pluripotent stem cell lines. *Stem Cell Rep.* 2015;4(4):591-604.
- Stock AA, Manzoli V, De Toni T, et al. Conformal coating of stem cell-derived islets for beta cell replacement in type 1 diabetes. *Stem Cell Rep.* 2020;14(1):91-104.
- Zhu H, Li W, Liu Z, et al. Selection of implantation sites for transplantation of encapsulated pancreatic islets. *Tissue Eng Part B Rev.* 2018;24(3):191-214.
- Velazco-Cruz L, Goedegebuure MM, Maxwell KG, et al. SIX2 regulates human  $\beta$  cell differentiation from stem cells and functional maturation in vitro. *Cell Rep.* 2020;31(8):107687.
- Camunas-Soler J, Dai X-Q, Hang Y, et al. Patch-seq links single-cell transcriptomes to human islet dysfunction in diabetes. *Cell Metab.* 2020;5(5):1017-1031.
- Augsornworawat P, Maxwell KG, Velazco-Cruz L, et al. Single-cell transcriptome profiling reveals  $\beta$  cell maturation in stem cell-derived islets after transplantation. *Cell Rep.* 2020;32(8):108067.
- Danielsson A, Pontén F, Fagerberg L, et al. The human pancreas proteome defined by transcriptomics and antibody-based profiling. *PLoS One.* 2014;9(12):e115421.
- Veres A, Faust AL, Bushnell HL, et al. Charting cellular identity during human in vitro  $\beta$ -cell differentiation. *Nature.* 2019;569(7756):368-373.

34. Kim H-I, Yu JE, Park C-G, et al. Comparison of four pancreatic islet implantation sites. *J Korean Med Sci.* 2010;25(2):203-210.
35. Wang X, Maxwell KG, Wang K, et al. A nanofibrous encapsulation device for safe delivery of insulin-producing cells to treat type 1 diabetes [in eng]. *Sci Transl Med.* 2021;13(596).
36. Dorrell C, Schug J, Canaday PS, et al. Human islets contain four distinct subtypes of  $\beta$  cells. *Nat Commun.* 2016;7:11756.
37. Deeds M, Anderson J, Armstrong A, et al. Single dose streptozotocin-induced diabetes: considerations for study design in islet transplantation models. *Lab Anim.* 2011;45(3):131-140.
38. Kilic G, Alvarez-Mercado AI, Zarrouki B, et al. The islet estrogen receptor- $\alpha$  is induced by hyperglycemia and protects against oxidative stress-induced insulin-deficient diabetes. *PLoS One.* 2014;9(2):e87941.
39. Szot GL, Yadav M, Lang J, et al. Tolerance induction and reversal of diabetes in mice transplanted with human embryonic stem cell-derived pancreatic endoderm. *Cell Stem Cell.* 2015;16(2):148-157.
40. U.S. National Institute of Health. *A Safety, Tolerability, and Efficacy Study of VX-880 In Participants With Type 1 Diabetes.* Accessed July 21, 2021. <https://clinicaltrials.gov/ct2/show/NCT04786262?term=vx-880&draw=2&rank=1>.
41. U.S. National Institute of Health. *A Study to Evaluate Safety, Efficacy, and Efficacy of VC-01 in Subjects With T1 Diabetes Mellitus (VC01-103).* Accessed July 21, 2021. <https://clinicaltrials.gov/ct2/show/NCT04678557>.
42. Cunha GR, Baskin L. Use of sub-renal capsule transplantation in developmental biology. *Differentiation.* 2016;91(4-5):4-9. <https://doi.org/10.1016/j.diff.2015.10.007>
43. Jofra T, Galvani G, Georgia F, et al. Murine pancreatic islets transplantation under the kidney capsule. *Bio-Protocol.* 2018;8(5):e2743.
44. Desai T, Shea LD. Advances in islet encapsulation technologies. *Nat Rev Drug Discov.* 2017;16(5):338-350.
45. Yu M, Agarwal D, Korutla L, et al. Islet transplantation in the subcutaneous space achieves long-term euglycaemia in preclinical models of type 1 diabetes. *Nat Metab.* 2020;2(10):1013-1020.
46. U.S. National Institute of Health. *A Safety, Tolerability and Efficacy Study of Sernova's Cell Pouch™ for Clinical Islet Transplantation.* Accessed July 21, 2021. <https://www.clinicaltrials.gov/ct2/show/NCT03513939>.
47. Haller C, Piccand J, De Franceschi F, et al. Macroencapsulated human iPSC-derived pancreatic progenitors protect against STZ-induced hyperglycemia in mice. *Stem Cell Rep.* 2019;12(4):787-800.
48. Kumagai-Braesch M, Jacobson S, Mori H, et al. The TheraCyte™ device protects against islet allograft rejection in immunized hosts. *Cell Transplant.* 2013;22(7):1137-1146.
49. Faleo G, K L, Nguyen V, et al. Assessment of immune isolation of allogeneic mouse pancreatic progenitor cells by a macroencapsulation device. *Transplantation* 2016;100(6):1211-1218.
50. Nyitray CE, Chang R, Faleo G, et al. Polycaprolactone thin-film micro- and nanoporous cell-encapsulation devices. *ACS Nano.* 2015;9(6):5675-5682.
51. Chang R, Faleo G, Russ HA, et al. Nanoporous immunoprotective device for stem-cell-derived  $\beta$ -cell replacement therapy. *ACS Nano.* 2017;11(8):7747-7757.
52. D A, Chiu A, Flanders JA, et al. Designing a retrievable and scalable cell encapsulation device for potential treatment of type 1 diabetes. *Proc Natl Acad Sci USA.* 2018;115(2):E263-e272.
53. Motté E, Szepessy E, Suenens K, et al. Composition and function of macroencapsulated human embryonic stem cell-derived implants: comparison with clinical human islet cell grafts. *Am J Physiol Endocrinol Metab.* 2014;307(9):E838-E846.
54. Izadi Z, Hajizadeh-Saffar E, Hadjati J, et al. Tolerance induction by surface immobilization of Jagged-1 for immunoprotection of pancreatic islets. *Biomaterials.* 2018;182:191-201.
55. Lanza R, Russell DW, Nagy A. Engineering universal cells that evade immune detection. *Nat Rev Immunol.* 2019:1-11.
56. Ameri J, Borup R, Prawiro C, et al. Efficient generation of glucose-responsive beta cells from isolated GP2+ human pancreatic progenitors. *Cell Rep.* 2017;19(1):36-49.